Simulation and Applications of Nonlinear Fiber Bragg Gratings

FARZIN EMAMI and AMIR H. JAFARI

Optoelectronic Research Center, Department of Electrical and Electronic Engineering,
Shiraz University of Technology
Airport Boulevard, Shiraz
IRAN

emami@sutech.ac.ir a.h.jafari@sutech.ac.ir
http://www.sutech.ac.ir

Abstract: - We have simulated the behaviors of nonlinear fiber Bragg gratings (FBGs). The generalized nonlinear equations governing these structures are solved by a method which uses a Fourier series procedure and a simple iterative method. All of the nonlinear effects are considered. Bragg soliton generation in intrinsic media and birefringence effects in FBGs are studied. We found that the first order dispersion can causes time shifting in the input pulse peak. It is shown that FBGs are proper for optical switching too. They can use in filters, nonlinear fiber optical applications, soliton propagations etc.

Key-Words: - Nonlinear Fiber Bragg gratings, Modulation intensity, Solitons, Birefringence, Optical switches, Simulation

1 Introduction

Application of a special type of the periodic structures called fiber Bragg gratings (FBGs) are introduced for about three decades [1], [2]. They have many applications in the optical communications such as optical filters, couplers, reflectors, dispersion comparators, etc [3], [4]. FBGs are consisting of a periodic modulation of the medium refractive index, along the core of the fiber [5], which has a short length that reflects particular wavelengths of light and transmits all others. In other words, they can be used as an inline optical filter to reject specific frequencies (frequency selector mirrors). Generally, the refractive index variations can be uniform or apodized [1], but usual structures for FBGs are:

- *uniform index gratings;*
- *apodized structures;*
- *chirped grating, and*
- *phase-shifted gratings.*

An attractive aspect of FBGs is the narrow bandwidth of them which can be used in an optical fiber [6], as notch filters. The large dispersive behaviors of these structures make them good devices for linear dispersion comparators, optical add/drop multiplexers (OADM) [7] in wavelength division multiplexing (WDM) systems [3] and optical multiplexers-demultiplexers with an optical circulator. Propagation of solitons is another application of FBGs. Nonlinear pulse propagation and compression, have been also reported in short period FBGs [8]-[10]. Due to the existence of a stop band in the transmission spectrum of FBGs, known as a photonic band gap (PBG), the nonlinear pulse propagation has many applications (such as an optical switch) in them.

For a medium with some nonlinearity, propagation of the waves is possible even though its frequency lies within the stop band such as Bragg solitons in the case of Kerr nonlinearity. Description of pulse propagation is based on a set of non-integrable nonlinear coupled (and maybe non-usual such as found in [11]) partial differential equations. They have solitary wave solutions.

In this paper, at first we review a general theory of FBGs. Then, in Section 2, the soliton propagation is discussed in the FBGs and the results of pulse propagation in these structures will be shown. In Section 3, the grating solitons are introduced. Bragg soliton generations are considered in Section 4. Important phenomenon called birefringence in fibers will be the next section contents. Section 6 belongs to a brief review of instabilities in the steady state response of the propagated pulse due to modulation instability parameter. FBG applications are subject of Section 7 and finally, conclusions are presented in Section 8.

2 FBG Formulation

A simple grating used in a FBG is shown in Fig.1

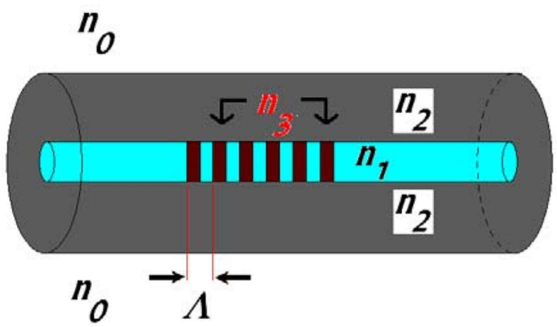

Fig. 1. A simple grating

The waves propagated in this medium id diffracted. For the incident angle θ_i the reflected angle θ_r we have [1]:

$$sin(\theta_i) - sin(\theta_r) = m\lambda = \overline{n}\Lambda \tag{1}$$

where Λ is the grating period and $\lambda / \overline{n}$ is the medium wavelength with the medium index of $\overline{n}$.

For the incident and the diffracted wave numbers, k_i and k_d, there is a relation with the grating wave number $k_g = 2\pi\Lambda$, as:

$$k_i - k_g = mk_g \tag{2}$$

If the incident light be in the fiber axis direction, using (1) we have:

$$\lambda = 2\overline{n}\Lambda \tag{3}$$

This is the Bragg condition [1].

To study the nature of forward and backward waves we can solve the Helmholtz equation considering the periodic variations of the grating refractive index, $\delta n_g(z)$, in the form of a Fourier series as:

$$\delta n_g(z) = \sum_{n=-\infty}^{+\infty} \delta n_n \exp(2\pi i n (z/\Lambda)) \tag{4}$$

Defining the forward and backward electric field amplitudes as A_f and A_b respectively, one can write the governing FBG equations in a coupled form of:

$$\begin{aligned} & i\frac{\partial A_f}{\partial z} + \frac{i}{v_g}\frac{\partial A_f}{\partial t} + \delta A_f + \kappa A_b \\ & \quad + \gamma\left(|A_f|^2 + 2|A_b|^2\right)A_f = 0 \\ & i\frac{\partial A_b}{\partial z} + \frac{i}{v_g}\frac{\partial A_b}{\partial t} + \delta A_b + \kappa A_f \\ & \quad + \gamma\left(|A_f|^2 + 2|A_b|^2\right)A_b = 0 \end{aligned} \tag{5}$$

Where δ is the detuning factor, v_g is the pulse group velocity, κ is the coupling coefficient and γ expresses the amount of the medium nonlinearity due to self-phase modulation (SPM) and cross-phase modulation (XPM) which defines as $\gamma = \frac{n_2\omega_0}{cA_{eff}}$; so A_{eff} is the effective area and n_2 is the nonlinear coefficient of the fiber medium. When a pulse propagates in a fiber, two cases may be considered; the linear case with $\gamma = 0$, and the nonlinear case with $\gamma \neq 0$. In the linear case with a CW operation of pulse the above equations will be:

$$\begin{aligned} & i\frac{\partial A_f}{\partial z} + \delta A_f + \kappa A_b = 0 \\ & i\frac{\partial A_b}{\partial z} + \delta A_b + \kappa A_f = 0 \end{aligned} \tag{6}$$

One solution of (6) can be written as:

$$\begin{aligned} & A_f(z) = A_1 \exp(i\,q\,z) + r\,B_2 \exp(-i\,q\,z) \\ & A_b(z) = B_2 \exp(-i\,q\,z) + r\,A_1 \exp(i\,q\,z) \end{aligned} \tag{7}$$

where $q = \pm\sqrt{\gamma^2 - \kappa^2}$ and $r = -\frac{\kappa}{\delta + q}$.

The relation between δ/κ and q/κ are plotted in Fig.2; this is the dispersion curve.

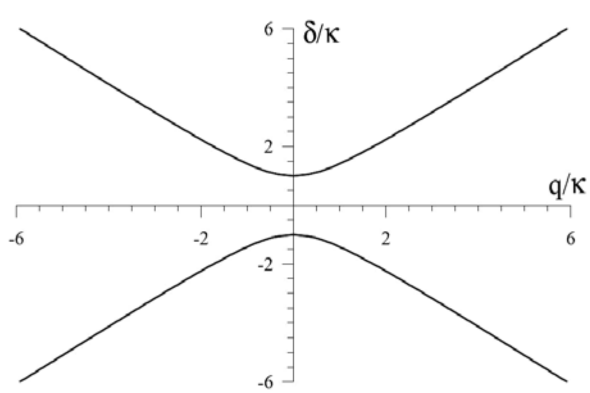

Fig. 2. Relation between detuning and q

When $-\kappa < \delta < \kappa$ the q-value is purely imaginary, we have a reflected wave from FBG and this is called a *photonic band-gap* too. For $|\delta| > \kappa$ the wave would be passed entirely from the grating.
The reflectance spectrum and the transmission factor of FBGs can be derived from (1) using the proper boundary conditions. In $z=L$ (where L is the grating length) after solving these equations the reflection coefficient will be:

$$r_g = \frac{i\,k\sin(qL)}{q\cos(qL) - i\,\delta\sin(qL)} \tag{8}$$

It is plotted in Fig. 3 for different detuning factor.

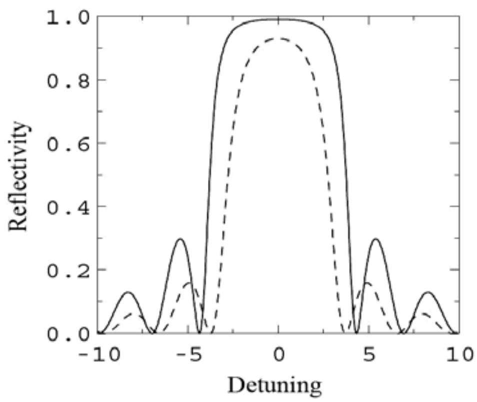

Fig. 3. FBG reflectivity versus the detuning factor

Due to dispersion effects in FBGs such as group velocity dispersion (GVD) and their increments especially around the stop band, there is a pulse broadening after the pulse propagation through the FBG. It will be serious near the band gap which has a more delay in pulse propagation. We simulate this broadening for a typical pulse propagated in a FBG and our results is seen in Fig. 4 [12].

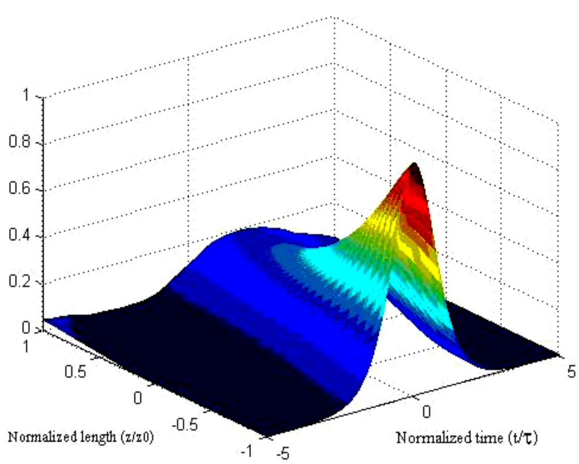

Fig. 4. Simulation of pulse propagation in FBG considering dispersion effects

Our simulation is based on a Fourier series expansion combined with a simple Jacobi iterative method (a predictor-corrector method) [12].
As you can see, there is an appreciable decrease in the pulse amplitude during its propagation.
For lower detuning the propagation delay increased and this is shown in Fig. 5.

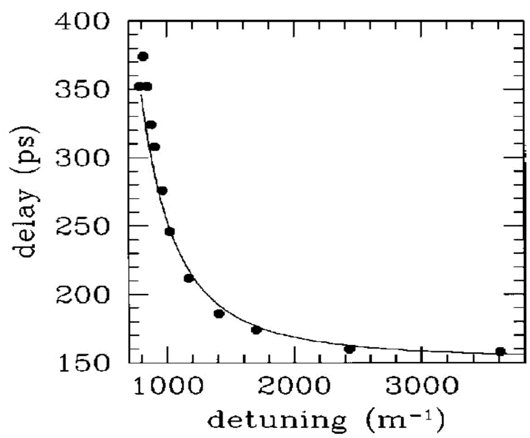

Fig. 5. Pulse propagation delay versus detuning

For nonlinear dispersion and in CW case we have the following relations for A_f and A_b:

$$A_f = u_f \exp(i\,q\,z)$$
$$A_b = u_b \exp(i\,q\,z) \tag{9}$$

If p_0 denotes the pulse power, two amplitudes u_f and u_b are:

$$u_f = \sqrt{\frac{p_0^2}{1+f^2}} \quad \& \quad u_b = \sqrt{\frac{p_0^2}{1+f^2}}\, f \tag{10}$$

where $f \equiv \frac{u_b}{u_f}$ & $P_0^{\;2} = u_f^{\;2} + u_b^{\;2}$.

Using (10) the values of δ and q are:

$$\delta = -\frac{k(1+f^2)}{2f} - \frac{3\gamma P_0}{2}$$
$$q = -\frac{k(1-f^2)}{2f} - \frac{\gamma P_0}{2}\frac{1-f^2}{1+f^2} \tag{11}$$

A plot of detuning versus q is shown in Fig. 6 [1].
Note for $|f| = 1$ the group velocity is zero and for $|f| > 1$ there is a negative group velocity which means the reflected waves.

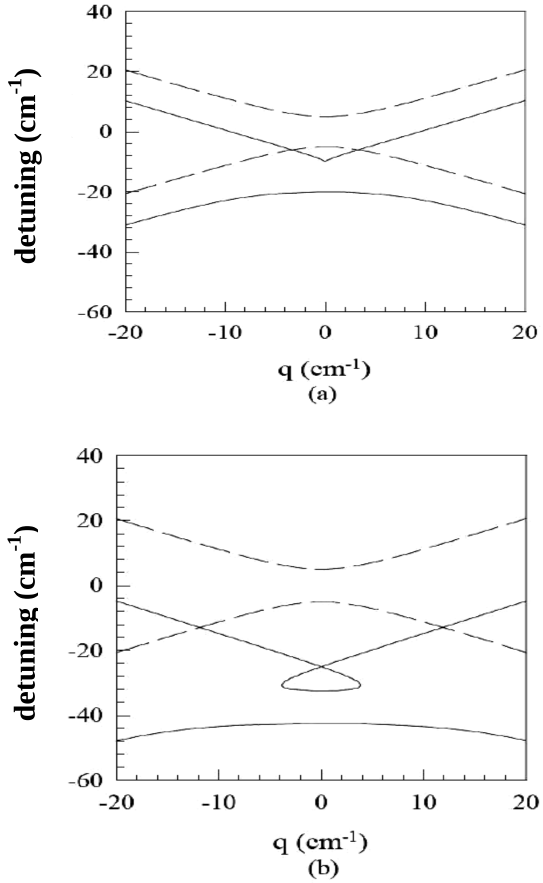

Fig. 6. A plot of detuning versus *q* for (a) $f < 0$, (b) $f > 0$; for $f = \pm 1$ we are on stop band exactly

3 Grating Solitons

As said, there are nonlinear effects in the fibers grating usually called Kerr effects, and for pulses propagated outside the band gap there is high dispersion. Kerr effect is the index dependency to the field strength I :

$$n = n_1 + n^{(2)} I$$

where n_1 is the background index and $n^{(2)}$ defines the amount of the medium nonlinearity.

In gratings, there are solitons which are the consequence of two mentioned effects; the Kerr effect and outside the band gap dispersion which are called the grating solitons [3], [4]. For solitons which have spectrum inside the photonic band gap we have gap solitons.

Since the amount of the dispersion in the grating are more than the usual fibers, there is a difference between the solitons in the grating and conventional fibers. In fact, the grating solitons are dens respect to the fiber solitons. Soliton analysis can be done using the coupled mode theory (CMT) [5], [6]. Utilizing the CMT, decompose the inside field of the grating as forward and backward parts E_f and E_b [7], [8]:

$$E = E_f(z, t_0)\exp(i(\beta_0 z - \omega_0 t)) + E_b(z, t)\exp(-i(\beta_0 z + \omega_0 t)) \quad (12)$$

After some mathematical manipulations and simplifications and using the Helmholtz equation the coupled equations derived as:

$$i\left[\frac{\partial E_f}{\partial z} + \frac{1}{v}\frac{\partial E_f}{\partial t}\right] + \kappa E_b \exp(-2i\delta z) + \gamma\left(|E_f|^2 + 2|E_b|^2\right)E_f = 0$$

$$-i\left[\frac{\partial E_b}{\partial z} - \frac{1}{v}\frac{\partial E_b}{\partial t}\right] + \kappa E_f \exp(2i\delta z) + \gamma\left(|E_b|^2 + 2|E_f|^2\right)E_b = 0 \quad (13)$$

where $v = \frac{c}{n_0}$ and κ, the coupling coefficient, is defined as $\pi n_1 / \lambda_0$. The detuning from the Bragg wavelength is $\delta = \frac{n_0}{c}(\omega_0 - \omega_B)$ and the nonlinear factor γ is $\frac{\pi n_2}{n_0 \lambda}$. As mentioned, the nonlinear terms contain the effects of SPM and XPM [10].

Operating at the Bragg frequency, the field components E_f and E_b satisfy the Klein-Gordon equation [10]:

$$\frac{\partial^2 E_f}{\partial z^2} - \frac{1}{v^2}\frac{\partial^2 E_f}{\partial t^2} = \kappa^2 E_f$$

$$-\frac{\partial^2 E_b}{\partial z^2} - \frac{1}{v^2}\frac{\partial^2 E_b}{\partial t^2} = \kappa^2 E_b \quad (14)$$

Assume $E_f = \exp(i(Kz - \Omega t))$; we have a dispersion equation for the structure such as:

$$K = \left(\left(\frac{\Omega}{v}\right)^2 - k^2\right)$$

K for all the frequencies of $\omega = \omega_B + \Omega$ between the frequency range of $\omega_B - \frac{\Delta\omega}{2} < \omega < \omega_B + \frac{\Delta\omega}{2}$, is a complex variable, with $\Delta\omega \equiv 2kc / n_0$.

To solve the equation for nonlinear case define:

$x = (k/2)(z + vt)$, $y = (\kappa/2)(z - vt)$,

$\sigma = \frac{\delta}{\kappa}$ and $U = (\frac{\gamma}{\kappa})^{0.5} E_f$;

we will have the following normalized equation:

$$i\frac{\partial U}{\partial x} + V\exp(-2i\delta(x+y)) + (|U|^2 + 2|V|^2)U = 0$$
$$-i\frac{\partial V}{\partial x} + U\exp(2i\delta(x+y)) + (|V|^2 + 2|U|^2)V = 0 \quad (15)$$

Neglecting SPM, for $\delta = 0$ the above equations are integrable and we can find their solitary equations using the Thirring model as [13]:

$$U = \hat{A}\,Sec^{1/2}(\tau/\tau_0)\exp(i\theta) \quad (16)$$

$$V = -\mu^2\hat{A}\,Sec^{1/2}(\tau/\tau_0)\exp(i\Phi) \quad (17)$$

with the following definitions:

$$\theta = \Psi_0 + \frac{1}{2}\frac{\mu^2 - 4\mu^4 - 3}{\mu^8 + \mu^4 + 1}\tan^{-1}[\sinh(\frac{\tau}{\tau_0})] \quad \&$$

$$\Phi = \Psi_0 + \frac{1}{2}\frac{3\mu^2 + 4\mu^4 - 1}{\mu^8 + 4\mu^4 + 1}\tan^{-1}[\sinh(\frac{\tau}{\tau_0})] \quad (18)$$

$$\hat{A} = \frac{4\mu^2}{\mu^8 + 4\mu^4 + 1}, \quad \tau = t - \frac{z}{v_e}, \quad \mu^4 = \frac{v - v_e}{v + v_e}$$
$$v_e = \pm\frac{v}{(1 + 4\kappa^2 v^2 \tau_0^{\,2})^{1/2}} \ \& \ \kappa^2 v^2 \tau_0^{\,2} = \frac{\mu^2}{\left(1 - \mu^4\right)^2} \quad (19)$$

With the aid of the above equations it is possible to have positive or negative solitons depends on the sign of $v - v_e$.

Now, the total waves inside the fiber can be written as:

$$E = (\frac{\kappa}{\gamma})^{1/2}\hat{A}\,sec\,h^{1/2}(\tau/\tau_0)\{exp\,[i(\Theta + \beta_0 z)]$$
$$-\mu^2\,exp[i(\Phi - \beta_0 z)]\}\,exp(-i\varpi_0 t) \quad (20)$$

For $\mu \approx 1, |v_e| << |v|$ and we have a slow soliton.

When the nonlinear coefficients n_2 and n_1 be comparable, the Bragg filter would be transparent [14], [15]. Finally, forward and backward solitons are correspond to $\mu \to 0$ and $\mu \to \infty$ respectively.

4 Bragg Soliton Generations in Intrinsic Medium

We can generate the Bragg solitons [16]-[18] in an electro-magnetically induced transparency medium [19]. Such media have big Kerr coefficient (or a large amount of $Re\left[\chi^3\right]$ where the factor χ denotes the medium susceptibility), low absorption coefficient and photonic band-gap controllability [20]. The refractive index can be written as:

$$n^2(z) = 1 + \overline{\chi}_0 + \delta\chi\cos(2k_B z) + \chi^{(3)}|E_p|^2 \quad (21)$$

$\overline{\chi_0}$ is the background susceptibility and $\delta\chi$ (modulation depth) is its amplitude variations; they both are frequency dependent. So, depending on the input pulse frequency it is possible to change band-gap.

5 Birefringence Effects on FBGs

Birefringence (BRG) effects are usually occurred in all types of FBGs. This effect can divide the peak to two parts at the Bragg wavelength [20]. Since the Bragg wavelength depends on the grating period and the effective index, physical and environmental effects such as temperature, stress and stretching the fiber can change the fiber index as:

$$d\lambda_B = [2\lambda_{B,0}(\frac{\partial n_{eff}}{\partial P}) + 2n_{eff\,0}(\frac{\partial \lambda_B}{\partial P})]dP$$
$$[2\lambda_{B,0}(\frac{\partial n_{eff}}{\partial T}) + 2n_{eff\,0}(\frac{\partial \lambda_B}{\partial T})]dT \quad (22)$$

Where P and T are pressure and temperature respectively. The variations of the effective index cause BRG and this is due to the changes in propagation constants of the guided waves. The value of BRG along the z-axis is:

$$B = \frac{|n_{\|} + n_{\perp}|}{n_0} = B_0 + \frac{|\Delta n_{\|} + \Delta n_{\perp}|}{n_0} \quad (23)$$

n_0 is the initial core index, $n_{\|}$ and $n_{\perp}$ are the parallel and perpendicular indices [21]. Fig. 7 shows the Bragg wavelength variations for different polarizations.

Deriving the refractive index and hence the propagation constant, explain the reflectance spectrum of *distributed* FBGs. It is found that this spectrum has more than one peak in Bragg wavelength and decomposes perfectly for higher forces. The results are plotted in Fig. 8. Such specification can be used in sensors.

6 Modulation Instability (MI)

Consider a FBG, excited by CW input pulse. The related MI parameter can cause instabilities in the steady-state response, in spite of CW input.

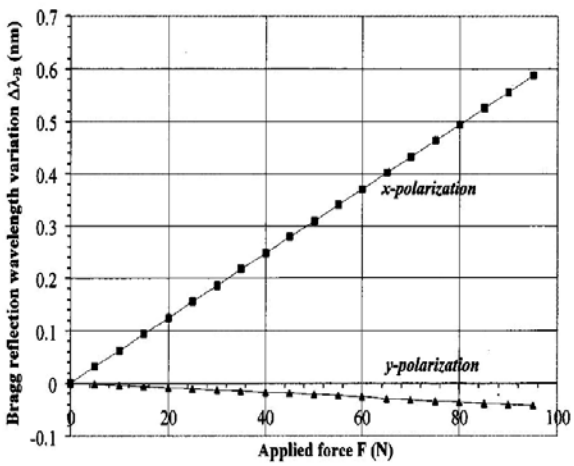

Fig. 7. The Bragg wavelength variations versus applied force

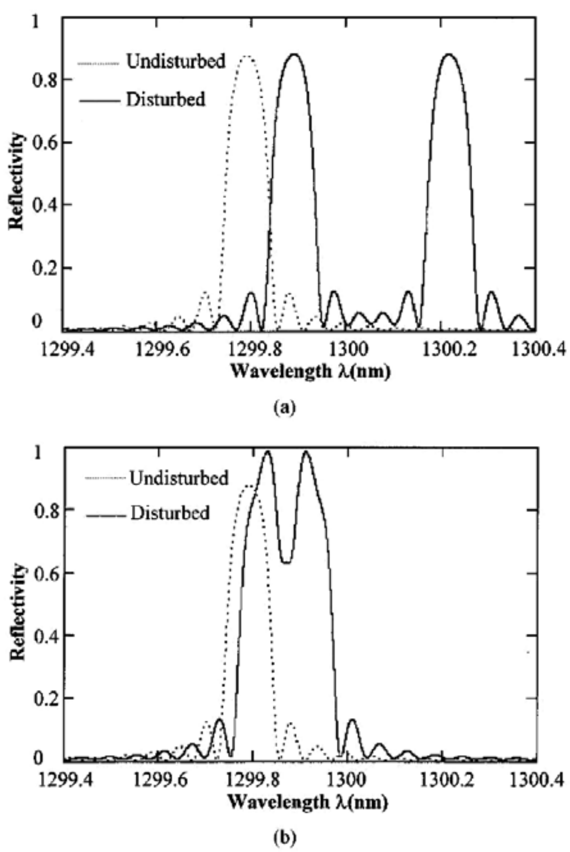

Fig. 8. The reflectivity as a function of the wavelength

This phenomenon is simulated using the coupled equations [5], and assuming a perturbation a_k imposed on input and output wave amplitudes modeled by:

$$A_k = (u_k + a_k)e^{iqz} \qquad k = f, b \tag{24}$$

Substitute (24) in the coupled equations and consider CW operation, we can derive a set of coupled equations for these perturbed terms as [23]:

$$i\frac{\partial a_f}{\partial z} + \frac{i}{v_g}\frac{\partial a_f}{\partial t} + \kappa a_f - \kappa f a_f + T\Big((a_f + a^*{}_f) + 2f(a_b + a_b{}^*)\Big) = 0$$
$$-i\frac{\partial a_b}{\partial z} + \frac{i}{v_g}\frac{\partial a_b}{\partial t} + \kappa a_b - \kappa f a_b + T\Big((a_b + a^*{}_b) + 2f(a_f + a_f{}^*)\Big) = 0 \tag{25}$$

where $T = \frac{\gamma P_0}{1 + f^2}$ is the effective nonlinear coefficient.

Select the following relations for these perturbing terms:

$$a_k = c_k \exp(i(Kz - \Omega t)) + d_k \exp(-i(Kz + \Omega t)) \tag{26}$$

Substitute (26) in (25), to have non-trivial solutions for a_k we derive the following transcendental equation:

$$(s^2 - K^2)^2 - 2\kappa^2(s^2 - K^2) - \kappa^2 f^2 (s + K)^2 - \kappa^2 f^{-2}(s - K)^2 - 4\kappa\Gamma f(s^2 - 3K^2) = 0 \tag{27}$$

where $s \equiv \frac{\Omega}{v_g}$. Here, we assume that the MI gain is equal to $2\,Im(S_m)$; where S_m is the root with the largest imaginary part.

The gain values for various δ are plotted in Fig. 9 and Fig. 10 [1]. As shown, for anomalous dispersion there is some gain even in $\delta = 0$ and it is possible to have instabilities. But, for normal GVD the MI gain is zero at $\delta = 0$ and we have stable conditions.

The instable conditions and gain spectrum are studied in FBGs with non-Kerr nonlinearities [23]. In a nonlinear medium we can write the forward and backward waves as [24]:

$$i\frac{\partial E_f}{\partial z} + \frac{i}{v_g}\frac{\partial E_f}{\partial t} + \delta E_f + \kappa E_b + \alpha_1(\frac{1}{2}|E_f|^2 + |E_b|^2)E_f - \alpha_2(\frac{1}{4}|E_f|^4 + \frac{3}{2}|E_f|^2|E_b|^2 + \frac{3}{4}|E_f|^4)E_f = 0$$

$$-i\frac{\partial E_b}{\partial z} + \frac{i}{v_g}\frac{\partial E_b}{\partial t} + \delta E_b + \kappa E_f + \alpha_1(\frac{1}{2}|E_b|^2 + |E_f|^2)E_b - \alpha_2(\frac{1}{4}|E_b|^4 + \frac{3}{2}|E_b|^2|E_f|^2 + \frac{3}{4}|E_f|^4)E_b = 0 \tag{28}$$

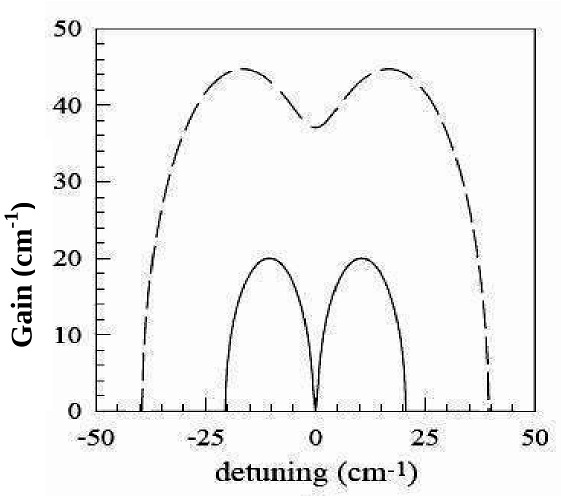

Fig. 9. A plot of gain versus *detuning* for anomalous dispersion

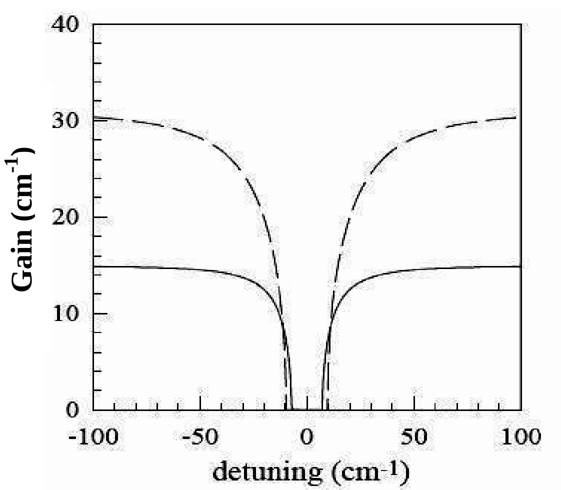

Fig. 10. A plot of gain versus *detuning* for normal dispersion

Assuming the disturbance terms in the form of:

$(u_j + a_j)e^{iqz}, \qquad |a_j| << u_j$

we have:

$$
\begin{aligned}
& i\frac{\partial a_f}{\partial z} + \frac{i}{v_g}\frac{\partial a_f}{\partial t} + \kappa a_b - \kappa f a_f \\
& + \frac{\Gamma_1}{2}((a_f + a_f^*) + 2(a_b + a_b^*)) \\
& - \Gamma_2\,\alpha_2(\frac{1}{4}(a_f + 2a_f^*) + \frac{3}{2}f(a_f + a_f^*) + \frac{3}{2}f^2(a_f + a_f^*) \\
& + \frac{3}{2}f^3(a_f + a_f^*) + \frac{1}{2}f^4 a_f) = 0
\end{aligned}
\tag{29}
$$

Define $G \equiv |Im[S_m]|$ and using (28) we can compute the gain-coupling relation. In this case, it is possible to have instability for anomalous dispersion whereas for normal dispersion there is a lower possibility for instability.

7 Grating Applications

In the nonlinear cases, FBGs are the bistable devices and we can use them as all-optical-switches. There are many methods to design such switches; self-induced nonlinear switches [25], AND-gate switches [26], pump-induced switches [27] and surface relief effects (in photo-polymer) [28]. All-optical switches are introduced in 1990 for the first time [29]. Gap-solitons are examples of FBG switching (self-switching in the pulse-propagation case). In these switches, the output energy of FBG increases with the pulse power (about %30-%40). Simulation results of these effects are plotted in Fig. 11.

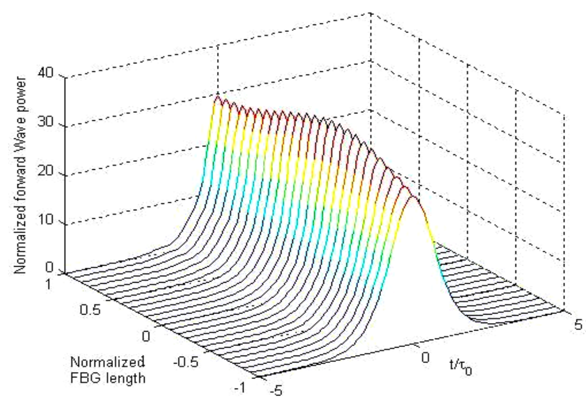

(a)

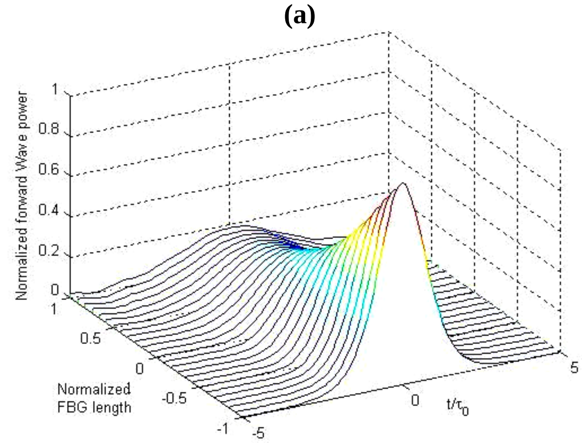

(b)

Fig. 11. Simulation results of the switching effects in a FBG; (a) high power pulse, (b) low power pulse

For lower energy cases, the wavelength lies in the stop-band and the coupling coefficient are grater than the detuning, so the pulse attenuates and FBG acts as a filter. Increasing the pulse energy can generate the nonlinear effects and the output energy raise. It is possible to see the gap-solitons if we use the pulse with higher energies. In other words, the energy transfer is done for high energy pulses, using gap-solitons.

AND-gates are another application of gap-solitons in the gratings [26], [30]. In these types of switches, there are two-orthogonal polarized pulses for two bits, where their frequencies are lying in the band-gap of the FBG. High and low energy output pulses correspond to bit '1' and '0' respectively. This is shown in Fig. 12.

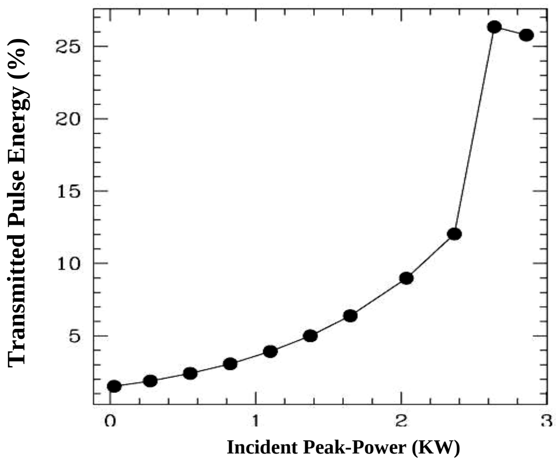

Fig. 12. Power dependence of the AND-gate

Nonlinear XPM effects are the other switching applications of FBGs [31]-[34]. If we apply two pulses with low and high amplitudes into the fiber, the XPM effect can causes the pulse propagation through the fiber due to the index nonlinearities and detuning variations. We simulate this behavior and plotted it in Fig. 13.

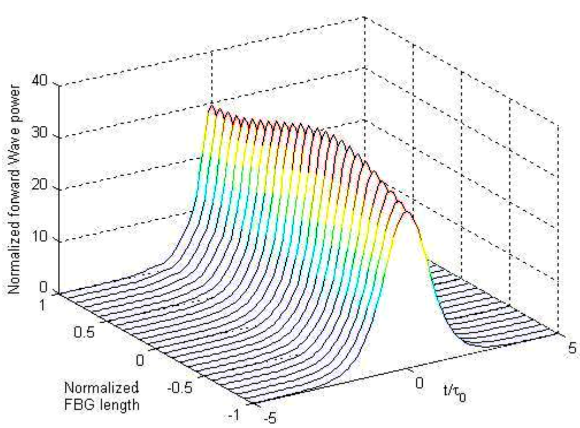

Fig. 13. Simulation of low-power pulse propagation, considering XPM

Grating couplers, which use the interactions of nonlinear Kerr effects on FBGs, are another application of FBGs [35]-[37]. In this switch, there is a four-port fiber with periodic-index variations along a central section of fiber with length L [38]-[40] for any incoming wave with wavelength of $\lambda = \lambda_B$, it will be reflected from port-2 and the other waves with the wavelengths nonequal to λ_B exit from port-4. Port-3 is an isolated port. In fact, there is a band-reject filter at the center of this coupler. XPM effects can change the grating index, for this case [41], [42].

Arrayed waveguide gratings (AWGs) are other usage of the grating, proper for optical filters and optical arrayed switches [43]. $1 \times N$ or $N \times N$ arrayed switches can be replaced for 1×2 or 2×2 switches (where cascading of them is a complicated process) [44]-[45]. Utilizing the AWG with polymeric materials, it is possible to design a temperature-sensitive $1 \times N$ or $N \times N$ switch [44].

Timing jitter tolerance can improved using a super structure FBG based rectangular pulse switching technology [46]. In this technique, the pulse shape converts from soliton to rectangular form.

8 Conclusion

In writing this article, we provide a glimpse of FBG theory and simulation. General description of FBG formulation and nonlinear propagation of solitons inside them are studied in brief. The nonlinear birefringence effects were introduced, distributed FBGs are considered and it was found that they can have applications in sensors. We hope our subjective selection of the above discussions along with the references reported here can present a general guideline in this area.

References:

[1] G. P. Agrawal, *Applications of Nonlinear Fiber Optics,* Acadamic press, 2001.

[2] B. J. Eggleton, C. M. de Sterke, and R. E. Slusher, "Bragg solitons in the nonlinear Schrödinger limit: experiment and theory," *J. Opt. Soc. Am. B,* Vol. 16, 1999, pp. 587-599.

[3] D. Taverner, N. G. R. Broderick, D. J. Richardson, M. Ibsen, and R. I. Laming, "All-optical and gate based on coupled gap-soliton formation in a fiber Bragg grating," *Opt. Lett.,* Vol. 23, 1998, pp. 259–261.

[4] D. Taverner, N. G. R. Broderick, D. J. Richardson, R. I. Laming, and M. Ibsen, "Nonlinear self-switching and multiple gap-soliton formation in a fiber Bragg grating," *Opt. Lett.,* Vol. 23, 1998, pp. 328–330.

[5] J. E. Sipe and H. G. Winful, ''Nonlinear Schrödinger solitons in a periodic structure,'' *Opt. Lett*., Vol. 13, 1988, pp. 132–133.

[6] C. M. de Sterke and J. E. Sipe, “Gap solitons,” in *Prog. in Opt.,* E. Wolf, ed., North-Holland, Amsterdam, 1994, Vol. 33, pp. 203–260.

[7] A. Othanos, and K. Kalli, *Fiber Bragg Gratings: Fundamentals and Applications in Telecommunications and Sensing,* Artech House, 1999.

[8] D. N. Christodoulides, and R. I. Joseph, “Slow Bragg solitons in nonlinear periodic structure”, *Phys. Rev. Lett*., Vol. 62, No. 15, 1989, pp. 1746-1749.

[9] H. Kogelnik and C. V. Shank, “Stimulated emission in a periodic structure,” *Appl. Phys. Lett.,* Vol. 18, 1971, pp. 152–154.

[10] H. G. Winful, in *Optical-fiber Transmission*, Ed. by E. Dash (Howward Sams, indianopolis, 1986), p 179.

[11] D. Zwillinger, Handbook of differential equations, 3rd Ed., Boston, MA: Academic Press, 1997.

[12] F. Emami, and A. H. Jafari, “Nonlinear fiber Bragg gratings,” *in Proc. Of the 8th WSEAS Int. Conf. on Microelectronics, Nanoelectronics, Optoelectronics,* Istanbul, Turkey, 2009, pp. 118-123.

[13] D.J. Kaup and A. C. Newell, “On the Coleman Correspondence and the Solution of the Massive Thirring Model,” *Lett. Al Nuvo Cimento*, Vol. 20, No. 9, 1977, pp. 325-331.

[14] W. Chen and D. L. Mills, “Gap solitons and the nonlinear optical response of super-lattices,” Phys. *Rev. Lett*., Vol. 58, 1987, pp.160-163.

[15] D. L. Mills and S. E. Trullinger, “Gap solitons in nonlinear periodic structures,” *Phys. Rev*. B 36, 1987, pp. 947–952.

[16] S. E. Harris, “Electromagnetically induced transparency,” *Phys. Today*, 1997, pp. 36-42.

[17] E. Arimondo, “Coherent population trapping in laser spectroscopy,” *in Progress in Optics*, Vol. 35, E. Wolf, eds. North-Holland, Amsterdam, 1996, pp. 257-353.

[18] M. Fleischhauer, A. Imamoglu and J. P. Marangos, “Electromagnetically induced transparency: Optics in coherent media,” *Rev. Mod. Phys*., 2005, Vol. 77, pp. 633-673.

[19] W. Jiang, Q. Chen, Y. Zhang and G. Guo, “Generating Bragg solitons in a coherent medium”, *Opt. Express,* Vol. 15, No. 13, 2007, pp. 7933-7939.

[20] S. E. Harris, J. E. Field and A. I. glu, ”Nonlinear optical processes using electromagnetically induced transparency”, *Phys. Rev. Lett*., Vol. 64, 1990, pp. 1107-1110.

[21] R. B. Wagreich, W. A. Atia, H. Singh, and J. S. Sirkis, “Effects of diametric load on fiber Bragg gratings fabricated in low birefringence fiber,’’ *IEE Electron*. *Lett*., Vol. 32, 1996, pp.1223-1224.

[22] R. Gafsi and M. A. El-Sherif “Analysis of Induced-Birefringence Effects on Fiber Bragg Gratings,” *Opt. Fiber Technol*., Vol. 6, 2000, pp. 299-323.

[23] K. Porsezian, K. Senthilnathan, and S. Devipriya, “Modulational Instability in Fiber Bragg Grating With Non-Kerr Nonlinearity”, *IEEE J. Quantum Elec.*, Vol. 41, 2005, pp. 789-796.

[24] J. Atai and B. A. Malomed, “Families of Bragg-grating solitons in a cubic-quintic medium,” *Phys. Lett. A*, Vol. 284, 2001, pp. 247–252.

[25] D. Taverner, N. G. R. Broderick, D. J. Richardson, M. Ibsen and R. I. Laming “Nonlinear Self-Switching an Multiple Gap Soliton Formation in a Fibre Bragg Grating," *Opt. Lett*., Vol. 23, 1998, pp. 328-330.

[26] D. Taverner, N. G. R. Broderick, D. J. Richardson, M. Ibsen and R. I. Laming “ All-Optical 'AND' Gate based on coupled Gap soliton formation in a Fibre Bragg Grating" *Opt. Lett.*, Vol. 23, 1998, pp. 259-261.

[27] N. G. R. Broderick, D. Taverner, D. J. Richardson, M. Ibsen and R. I. Laming “Optical pulse compression in fiber Bragg gratings," *Phys. Rev. Lett*. Vol. 79, 1997, pp. 4566-4569.

[28] K. Pavani, I. Naydenova, S. Martin,J. Raghavendra, R. Howard , V. Toal, “Electro-optical switching of liquid crystal diffraction gratings by using surface relief effect in the photopolymer”, *Opt. Comm.,* Vol. 273, 2007, pp. 367–369.

[29] S. LaRochelle, Y. Hibino, V. Mizrahi, and G. I. Stegeman, “All-Optical switching of Grating Transmission using Cross-Phase Modulation in optical fibers," *Elect. Lett*., Vol. 26, 1990, pp. 1459-1460.

[30] S. Lee and S.-T. Ho, “Optical switching scheme based on the transmission of coupled gap solitons in a nonlinear periodic dielectric media," *Opt. Lett.*, Vol. 18, 1993, pp. 962-964.

[31] G. P. Agrawal, P. L. Baldeck, and R. R. Alfano, “Temporal and spectral effects of cross-phase modulation on co-propagating ultra-short pulses in optical fibers ”,*Phys. Rev. A*, Vol. 40, 1989, pp. 5063.

[32] R. A. Saunders, B. L. Patel, H. J. Harvey, and A. Robinson, “Cross-phase modulation in an L-band EDFA” *Electron. Lett*,. Vol. 32, 1996, p. 2206.

[33] H. J. Thiele, R. I. Killey, V. Mikhailov and P. Bayvel, "Cross-phase modulation distortion in multi-span dense WDM systems," 11th Tyrrhenian Workshop on Digital Communications, Portofino, Italy, September 1999.

[34] R. Hui, K. R. Demarest, and C. T. Allen, "Cross-Phase Modulation in Multispan WDM Optical Fiber Systems," *IEEE J. Lightwave Technol*., Vol. 17, 1999, pp. 1018-1026.

[35] S. R. Friberg, Y. Silberberg, M. K. Oliver, M. J. Andrejco, M. A. Saifi and P. W. Smith, "Ultra-fast All-Optical Switching in a Dual Core Fibre Nonlinear Coupler", *App. Phys. Lett.,* Vol. 51, 1987, pp. 1135-1137.

[36] S. R. Friberg and P. W. Smith, "Nonlinear optical glasses for ultra-fast optical switches," *IEEE J. Quantum Electron*. Vol. 23, 1987, pp. 2089–2094.

[37] R. H. Stolen, and C. Lin, "Self-phase modulation in silica optical fibers," *Phys. Rev. A,* Vol. 17, 1987, pp. 1448–1453.

[38] K. O. Hill and G. Meltz, "Fiber Bragg grating technology fundamentals and overview," *IEEE J. Lightwave Technol*., Vol. 15, 1997, pp. 1263-1276.

[39] M. Yamada and K. Sukuda, "Analysis of almost-periodic distributed feedback slab waveguides via a fundamental matrix approach," *Appl. Opt.* Vol. 26, 1987, pp. 3474-3478.

[40] I. Bennion, J. A. R. Williams, L. Zhang, K. Sugden, and N. J. Doran, "UV-written in-fiber Bragg gratings," *Opt. Quantum Electron*., Vol. 28, 1994, pp. 93–135.

[41] G. P. Agrawal,, *Nonlinear Fiber Optics,* 2nd ed., Academic Press, New York, 1995, Chap.7.

[42] S. M. Jensen, "The nonlinear coherent coupler," *IEEE J. Quantum Electron*. Vol. 18, 1982, pp. 1580-1583.

[43] G. Hu, Y. Cui, B. Yun, C. Lu, Z. Wang., "A polymeric optical switch array based on arrayed waveguide grating structure", *Opt. Comm.*, Vol. 279, 2007, pp. 79-82.

[44] T. Goh, A. Himeno, M. Okuno, H. Takahashi, K. Hattori, "High-extinction ratio and low-loss silica-based 8×8 strictly non-blocking thermo-optic matrix switch," *IEEE J. Lightwave. Technol*., Vol. 17, 1999, pp. 1192-1199.

[45] T. Shibata, M. Okuno, T. Goh, T. Watanabe, M. Yasu, M. Itoh, M. Ishii, Y. Hibino, A. Sugita, A. Himeno, "Silica-based waveguide-type 16/spl times/16 optical switch module incorporating driving circuits," *IEEE Photon. Technol. Lett*., Vol. 15, 2003, pp. 1300-1302.

[46] J. H. Lee, L. K. Oxenløwe, M. Ibsen, K. S. Berg, A. T. Clausen, D. Richardson, and P. Jeppesen, "All-Optical TDM data de-multiplexing at 80 Gb/s with significant timing jitter tolerance using a fiber Bragg grating based rectangular pulse switching technology," *IEEE J. Lightwave Technol*., Vol. 21, pp. 2518-2533, 2003.